

Investigation of Fixed Neutron Source Effect in Dynamic Control Rod Reactivity Measurement Method

YuGwon Jo*, Hwan-Soo Lee, and Eun-Ki Lee

Korea Hydro & Nuclear Power Co., Ltd. Central Research Institute,
70, Yuseong-daero 1312beon-gil, Yuseong-gu, Daejeon, Korea 34101
*yugwonjo@khnp.co.kr

1. Introduction

The dynamic control rod reactivity measurement (DCRM) method has been successfully applied to 2,600 rod bank worths of the pressurized water reactors (PWRs) in Korea since 2006 [1]. Recently, a modified DCRM method named as DCRM-EK (Equilibrium-kinetics status) has been developed to overcome the low-sensitivity of the pulse counts obtained from the integral fission chamber and demonstrated its validity through the preliminary test results [2]. The DCRM-EK makes the best use of the linear range of the pulse count by starting the rod insertion from the critical state at the maximum count rate before the pulse pile-up, where the test rod is initially inserted with around 70 pcm to maintain the criticality. Since the DCRM-EK utilizes the measured critical position, the on-site generation of the design constants for the DCRM by the three-dimensional (3-D) nodal kinetics calculations is required.

On the other hand, the DCRM design constants which are the point-kinetics (PK) parameters, the neutron-to-response conversion factor (NRCF), and the dynamic-to-static conversion factor (DSCF) are generated by the 3-D nodal kinetics calculation neglecting the fixed neutron source. Since there always exist the fixed neutron sources from the reloaded fuels or from the external neutron sources to provide the minimum count rate for the ex-core detector, there is a discrepancy between the 3-D simulation and the real core.

Recently, the internal neutron source calculation capability has been implemented in the RAST-K v2 [3] and applied to the low-power transient analysis [4]. This paper investigates the fixed neutron source effect in the DCRM design constants and the dynamic reactivity obtained by the inverse-point kinetics calculation.

2. Internal Neutron Source Calculation

This section briefly describes the internal neutron source calculation capability of RAST-K v2. A more detailed information can be found in Ref. [4]. The internal source emitted from the depleted fuel comprises of the spontaneous fission source and the (α, n) neutron source. The node-wise spontaneous fission source can be calculated as:

$$S_{sf}^m = \sum_i \nu_i f_{sf}^i \lambda_i N_i^m, \quad (1)$$

where i is the nuclide index, m is the node index, λ_i is the decay constant, f_{sf}^i is the branching ratio for the spontaneous fission, ν_i is the neutron yield per spontaneous fission, and N_i^m is the number density of nuclide i at node m .

The RAST-K v2 calculates the node-wise (α, n) neutron sources based on the average alpha energy \bar{E}^i instead of the detailed alpha energy spectrum as Eq. (2):

$$S_{(\alpha, n)}^m = \sum_i S_{\alpha}^{m, i} y^m(\bar{E}^i), \quad (2a)$$

$$S_{\alpha}^{m, i} = \lambda_i f_{\alpha}^i N_i^m, \quad (2b)$$

where $S_{\alpha}^{m, i}$ is the alpha source intensity emitted from nuclide i at node m , f_{α}^i is the alpha decay branching ratio, and the $y^m(\bar{E}^i)$ is the neutron yields at node m induced by the (α, n) reactions of an alpha particle emitted with energy \bar{E}^i .

To calculate $y^m(E)$, Ref. [5] proposed to approximate the alpha stopping cross section by the Alsmiller-Estabrook correlation [6] for the computational efficiency. By adopting this strategy, the $y^m(E)$ can be calculated as:

$$y^m(E) = \omega^m \sum_i N_i^m \tau_i(E), \quad (3)$$

where $\tau_i(E)$ indicates the microscopic integral neutron production by the (α, n) reaction and the ω^m is the slowing-down parameter at node m , which can be calculated, respectively, as:

$$\tau_i(E) = \int_0^E \sigma_{(\alpha, n)}^i(E') \sqrt{E'} dE', \quad (4a)$$

$$\omega^m = 1 / \left(1.866 \times 10^{13} \sum_i N_i^m \sqrt{Z_i} \right), \quad (4b)$$

where $\sigma_{(\alpha, n)}^i(E)$ is the microscopic (α, n) cross section of nuclide i , Z_i is the atomic number of nuclide i , and E is the alpha energy (eV). It should be noted that $\tau_i(E)$ can be pre-calculated and tabulated for \bar{E}^i to reduce the computational burdens for the numerical integration in Eq. (4a). Compared to the ORIGEN(v6.1), the (α, n) neutron source calculation algorithm implemented in RAST-K v2 showed an error less than 1%, where the error is mainly caused by the Alsmiller-Estabrook correlation [4].

3. DCRM Design Constants

The time-dependent two-group nodal balance equations with the fixed neutron source can be written as:

$$\frac{1}{v_g} \frac{d\phi_g^m(t)}{dt} = R_g^m + S_{fixed,g}^m \text{ for } g = 1, 2, \quad (5)$$

where $\phi_g^m(t)$ is the neutron flux in group g at node m and v_g is the average neutron speed in group g , R_g^m is the net neutron production rate except for the fixed source, and $S_{fixed,g}^m$ is the fixed neutron source defined as:

$$S_{fixed,1}^m = S_{sf}^m + S_{(\alpha,n)}^m, \quad (6a)$$

$$S_{fixed,2}^m = 0, \quad (6b)$$

In Eqs. (6a) and (6b), the fixed neutron source is considered as fast group, since the average neutron energies from the (α,n) reaction and the spontaneous fission are 2.55 and 2.10 MeV, respectively for a typical depleted fuel.

Then, one can derive the PK equations from Eq. (5) as:

$$\frac{dn(t)}{dt} = \frac{\rho(t) - \beta(t)}{\Lambda(t)} n(t) + \sum_{k=1}^6 \lambda_k(t) C_k(t) + S_{fixed}, \quad (7a)$$

$$\frac{dC_k(t)}{dt} = \frac{\beta_k(t)}{\Lambda(t)} n(t) - \lambda_k(t) C_k(t), \quad (7b)$$

where $\rho(t)$ is the dynamic reactivity, $\beta_k(t)$, $\lambda_k(t)$, and $\Lambda(t)$ are the PK parameters, which are following the conventional definitions. These quantities can be obtained from the 3-D nodal kinetics calculations with an appropriate temporal discretization. Similar to the PK parameters, the reduced fixed source density S_{fixed} in Eq. (5) can be obtained as:

$$S_{fixed} = \frac{\sum_{m=1}^M V^m \sum_{g=1}^2 W_g^m S_{fixed,g}^m}{\sum_{m=1}^M V^m \sum_{g=1}^2 W_g^m}, \quad (8)$$

where V^m is the volume of node m and W_g^m is the arbitrary weighting function. Based on the first-order perturbation theory, it is a standard to select the weighting function as the adjoint flux Φ_g^T at the initial steady state. However, the constant weighting function (e.g., $W_g^m = 1$) was also investigated for comparison.

From the 3-D nodal kinetics calculations, the NRCF and the DSCF can be obtained, respectively, as:

$$NRCF^Q = \frac{\bar{R}^Q(t)}{\bar{n}(t)} \text{ for } Q = \text{bottom, middle, top}, \quad (9)$$

$$DSCF = \frac{\rho_{static}}{\rho_{dynamic}}, \quad (10)$$

where $\bar{R}^Q(t)$ is the normalized detector response for the detector at Q , \bar{n} is the normalized core-averaged neutron density (CAND), ρ_{static} is the static rod worth obtained from the k-eigenvalue calculations, $\rho_{dynamic}$ is the dynamic reactivity of the test rod when the test rod is fully inserted.

In this study, the delayed neutron source effect is not considered for the static rod worth, since it is just a nominal quantity to compare the measured static rod worth with the designed value in the nuclear data report (NDR).

4. Numerical Results

At first, the fixed neutron sources were calculated by RAST-K v2 on a typical PWR test problem shown in Fig. 1. Figure 2 shows the radial and axial distributions of the fixed sources. Since there is no external source and the internal sources are mainly emitted from the transuranic isotopes, the fixed source distributions are high in the core peripheral region where the twice-burned fuels are located and slightly bottom-skewed.

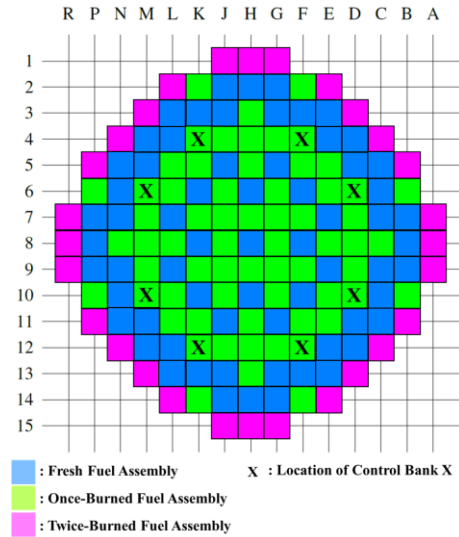


Figure 1. Configuration of a typical PWR test problem.

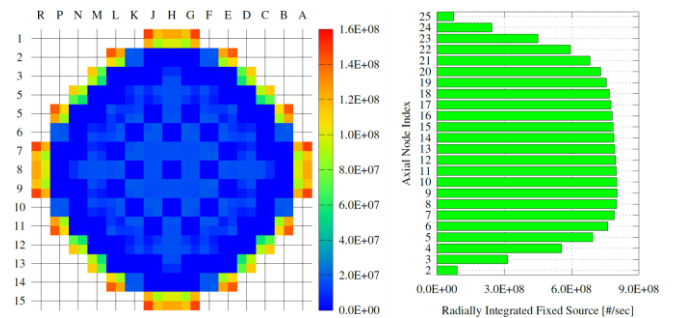


Figure 2. Axially-integrated node-wise radial distributions (left) and radially integrated node-wise axial distributions (right) of the fixed neutron sources.

Table I summarizes the internal fixed source information. The total fixed source intensity is calculated as $1.543\text{E}+10$ n/sec, where the spontaneous fission is dominant. The constant-weighted fixed source density is calculated by dividing total fixed source intensity by the entire core-reflector volume, while the adjoint-weighted fixed source density is calculated by Eq. (8) with the adjoint flux weighting function. The adjoint-weighted fixed source density is smaller than the constant-weighted value, which is due to the low adjoint flux in the core peripheral region.

Table I. Summary of internal fixed source information for a typical PWR test problem

	Value	Unit
Spontaneous Fission Source	1.404E+10	n/sec
(α ,n) Neutron Source	1.390E+09	n/sec
Total Fixed Source	1.543E+10	n/sec
Constant-Weighted Fixed Source Density	349.0	n/cm ³ -sec
Adjoint-Weighted Fixed Source Density	132.8	n/cm ³ -sec

The 3-D nodal kinetics calculations were performed with and without fixed source, where the transient scenario is as follows to maximize the fixed source effect. The reactor was initially steady-state for 60 seconds at the all-rod-out (ARO) condition. At the initial steady state, the reactor was critical state when there is no fixed source. However, it was slightly subcritical state in the presence of the fixed source. Then, the control rod bank X indicated in Figure 1 was fully inserted for 280 seconds and fully withdrawn right after the end of insertion for 280 seconds. From the 3-D kinetics calculations, the dynamic reactivity and the DCRM design constants were obtained.

Figure 3 compares the adjoint- and constant-weighted dynamic reactivities obtained from the 3-D kinetics calculations with and without fixed source. When adjoint flux is used for the weighting function, the dynamic reactivities show good agreement (less than 0.1%) regardless of the fixed source, while the constant-weighted dynamic reactivities show a significant difference when the control rod is at the fully inserted. The dynamic reactivity is insensitive to the presence of the fixed source when the adjoint flux is used for the weighting function, which shows the importance of the adjoint weighting for the PK model. From now on, only the results for the adjoint weighting function will be presented.

Figure 4 compares the adjoint-weighted CANDs obtained from the 3-D kinetics calculations with and without fixed source during the rod insertion, which shows that the CAND is insensitive to the presence of fixed source. Figure 5 compares the NRCFs with and without fixed source, where the differences in the NRCFs at the fully inserted condition are 3.75% and 1.37% for bottom and top detectors, respectively. The reason for the larger difference in the bottom detector may be due to the slightly bottom-skewed fixed source distribution. Figure 6 compares the adjoint-

weighted generation time and delayed neutron fraction with and without fixed source, where the negligible differences can be observed.

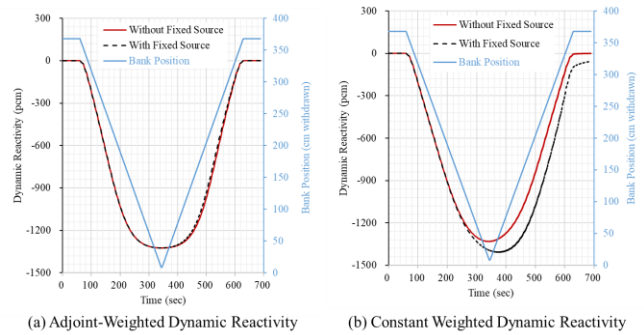


Figure 3. Comparisons of adjoint- and constant-weighted dynamic reactivities obtained with and without fixed source.

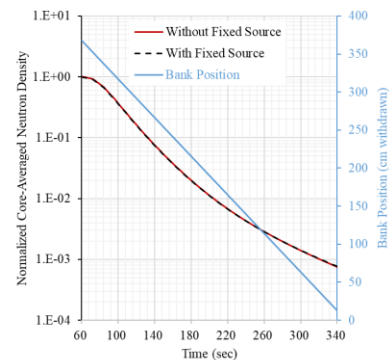


Figure 4. Comparisons of adjoint-weighted CANDs with and without fixed source.

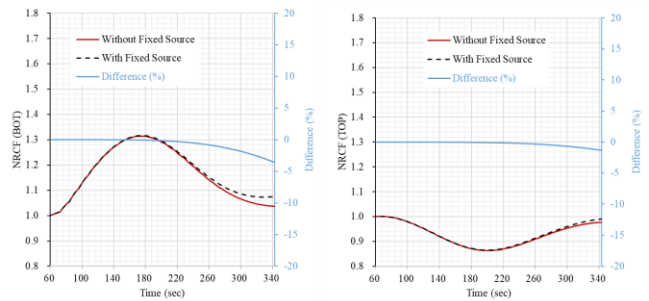


Figure 5. Comparisons of NRCFs for bottom (left) and top (right) detectors with and without fixed source.

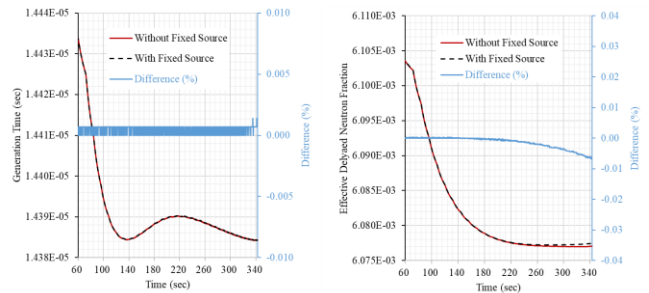


Figure 6. Comparisons of generation times (left) and delayed neutron fractions (right) with and without fixed source.

Table II compares the dynamic rod worths and the DSCFs obtained from the 3-D nodal calculations with and without fixed source, where the differences due to the fixed source are negligible.

Table II. Comparisons of dynamic rod worths and DSCFs with and without fixed source

Static Rod worth (pcm)		1286.12
Dynamic Rod worth (pcm)	Without Fixed Source	-1325.59
	With Fixed Source	-1324.24
DSCF	Without Fixed Source	0.97022
	With Fixed Source	0.97121
	Difference (%)	-0.10

Table III show the test cases for the sensitivity analysis of the dynamic reactivities from the inverse PK calculations, where the reference input signal is obtained from the detector response of the 3-D kinetics calculation with fixed source. The results are shown in Figure 7. Regardless of the presence of the fixed source in the 3-D calculation, an appropriate fixed source intensity for the inverse PK calculation leads to the accurate estimation of dynamic reactivity. It is noted that an iterative approach was introduced in cases A2 and B2 to update the fixed source intensity to satisfy the condition of zero slope at 620 second (ARO condition) and eliminate the reactivity overshoot observed in cases A1 and B1 in Figure 7. Please refer to the [7] for more detailed information. In cases A1 and B1, 41 pcm differences are observed at the fully inserted condition, while the difference is less than 1 pcm in other cases.

Table III. Test cases for sensitivity analysis of the dynamic reactivities from inverse PK calculations

Test Cases	Way to Generate DCRM Constants	Fixed Source Intensity for Inverse PK Method	
		Value (n/cm ³ -sec)	Way to Determine Fixed Source Intensity
Case A1	3-D Calculation with Fixed Source	0.0	No Fixed Source
Case A2	3-D Calculation with Fixed Source	134.8	Iteration to Eliminate Reactivity Overshoot at ARO
Case A3	3-D Calculation with Fixed Source	132.8	Adjoint Weighted Average of Fixed Source
Case B1	3-D Calculation without Fixed Source	0.0	No Fixed Source
Case B2	3-D Calculation without Fixed Source	134.8	Iteration to Eliminate Reactivity Overshoot at ARO
Case B3	3-D Calculation without Fixed Source	132.8	Adjoint Weighted Average of Fixed Source

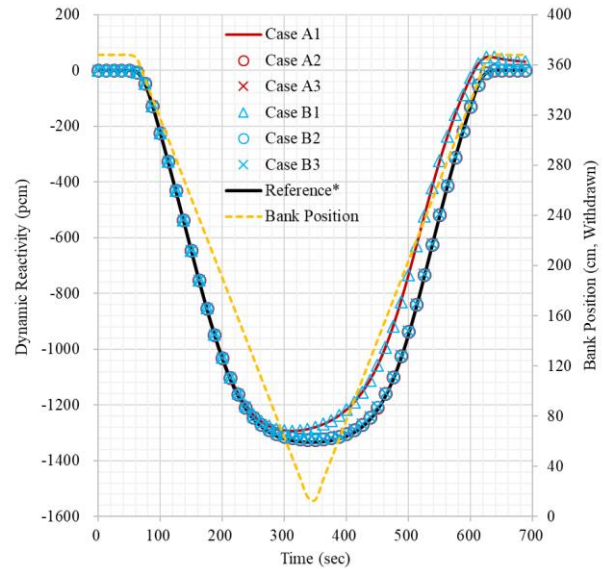


Figure 7. Sensitivity analysis results of the dynamic reactivities from inverse PK calculations; The reference is calculated by the 3-D kinetics calculation with fixed source.

5. Conclusions

In conclusions, the adjoint weighting function for the PK model significantly suppresses the impact of the fixed neutron to the 3-D dynamic reactivity, while a small difference in the reactivities obtained by the inverse PK calculations with and without fixed source can be observed. However, it can be also eliminated by an appropriate selection of the fixed source intensity as 100 n/cm³-sec.

REFERENCES

- [1] E.K. Lee, et al., "New Dynamic Method to Measure Rod Worths in Zero Power Physics Tests at PWR Startup," *Annals of Nuclear Energy*, Vol. 32, pp. 1457-1475 (2005).
- [2] E.K. Lee, et al., "Dynamic rod worth measurement method based on equilibrium-kinetics status," *Nucl. Eng. and Technol.*, Vol. 54, pp. 781-789 (2022).
- [3] J. Park, et al., "RAST-K v2 – Three-dimensional Nodal Diffusion for Pressurized Water Reactor Core Analysis," *Energies*, Vol. 13, p. 6324 (2020).
- [4] Y.G. Jo and H. C. Shin, "Low power transient analysis of PWR reload core with fixed neutron source via 3-D nodal diffusion code RAST-K," *Ann. Nucl. Energy*, Vol. 150, 107742(online reference number) (2021).
- [5] D.P. Griesheimer, et al., "In-Line (α,n) Source Sampling Methodology for Monte Carlo Radiation Transport Simulations," *M&C 2017*, Jeju, Korea, April 16-20, 2017.
- [6] F.S. Alsmiller, G.M. Estabrook, "Neutron Yields from (α,n) Reactions," ORNL-3016, pp. 242, Oak Ridge National Laboratory (1960).
- [7] G. Bogdan, "Dynamic Rod Worth Measurement ("Rod Insertion")," IAEA-R-7949-F, IAEA, December 1996.